Microwave and soft x-ray emission from solar flare events associated with coronal transients

I. M. Chertok, A. A. Gnezdilov, and E. P. Zaborova

Institute of Terrestrial Magnetism, the Ionosphere, and Radio Propagation, Russian Academy of Sciences

(Submitted May 21, 1991)

Astron. Zh. **69**, 593–603 (May–June 1992)

The properties of microwave and soft x-ray bursts accompanying coronal transients (CTs) detected by the P78-1 satellite are analyzed. It is shown that the distribution of events on "intensity–effective burst duration" diagrams enables one not only to distinguish between bursts with and without CTs, but also to determine the relationship between the burst characteristics and the main CT parameters (angular size, velocity, mass, and shape). Large high-velocity CTs of complicated shape are normally observed in combination with the most intense and prolonged bursts. Those with moderate parameters and a relatively simple shape are identified with moderate, unpulsed, soft x-ray and microwave bursts, as well as with radio bursts of the "gradual rise and fall" type. Most pulsed bursts are generally not accompanied by CTs, but the most intense ones may be associated with small CTs of simple shape. The relationship between CT eruption and flare energy release is discussed.

INTRODUCTION

Coronal transients (CTs) are large-scale ejections of solar plasma with mass $m \sim 10^{14}$-$3\cdot10^{16}$ g, characteristic size of several $R_\odot$, and velocity $V \sim 10^2$-$2\cdot10^3$ km/sec (see Refs. 1 and 2 and the bibliography therein). In observations with satellite coronagraphs in white light, CTs at heliocentric distances (2-10)$R_\odot$ often have a loop shape. They have also been detected as a curved front, a fan, halo, single, double, or multiple spikes, etc. Coronal transients are one of the fundamental phenomena of solar activity and play an important role in the most varied processes, from eruptive prominences, disappearing filaments, and flares to interplanetary disturbances and geomagnetic storms.

The eruption of a CT is accompanied by various kinds of electromagnetic radiation. Soft x-ray and microwave bursts are generated, in particular, in the region of development of a CT, in the upper chromosphere and lower corona. The shocks that are often observed in events with a CT are manifested, as they propagate in the corona, as slowly drifting, type II radio bursts at meter wavelengths. The energetic electrons trapped in magnetic traps within a CT or individual components of it produce continuum, broadband type IV radio emission. A detailed analysis of the electromagnetic emission from CTs is obviously of great interest for understanding the nature of CTs and their relationship to flare and flare-like energy release and other accompanying phenomena. Moreover, the laws characterizing the relationship between electromagnetic emission and the development of CTs with given parameters (angular size, velocity, mass, and shape) can serve as a basis for CT diagnostics and can be used in a system of solar–terrestrial prediction.

The relationship between CTs and soft x-ray bursts, for the most part, as well as types II and IV radio bursts in the meter range, has been considered in Refs. 3-7. It was shown, in particular, that events with CTs are most often characterized by long-duration events (LDEs) in soft x rays with a total duration $\tau \geq 1$ h, and the relationship between types II and IV radio bursts and CTs is not unique. Here we devote most of our attention to analyzing the relationship between CT parameters and the characteristics of microwave radio bursts, which reflect energy release in the forms of both plasma heating and accelerated particles. Another significant distinction of the present analysis is that a combination of the intensity and duration of emission is used as the main parameter for both microwave and soft x-ray bursts. In particular, the distribution in the "intensity–burst duration" plane of events with different CT characteristics turns out to be highly informative. It then becomes possible to identify and analyze the differences between pulsed flares, large prolonged bursts with complicated space–time structure, and events of the "gradual rise and fall" (GRF) type, and to determine the conditions of development of CTs with different parameters, particularly the angular size, velocity, shape, mass, etc.

A question now being widely debated is which comes first – the CT or the flare, i.e., is a CT a consequence of flare energy release or, does a CT eruption stimulate a flare (see Refs. 2 and 8)? We shall return to this problem in discussing the results of the present analysis. We now stress that in the text we must often apply words like "accompanied," "associated," "related," etc., to CTs and accompanying phenomena. These should not be considered to imply a definite cause-and-effect relationship between CTs and flares, however, except when explicitly stated.

INITIAL DATA

The analysis is based on data published in Refs. 4, 6, and 9-13 on about 110 CTs detected by the P78-1 satellite, using the SOLWIND coronagraph, from March 1979 to December 1982 and identified by the authors of the experiment with flares on the visible disk. Recall that CTs are recorded in projection onto the plane of the sky. Their true parameters can therefore be determined directly only in events that occur near the limb. That being the case, in comparing CT parameters with electromagnetic radiation below, we consider events associated with activity in the limb zone of heliolongitude $|l| \geq 45°$. Events from the central part of the disk can be used just to analyze the fact that a CT was formed in connection with some activity, without allowance for the observed CT parameters.

Since in the present paper we determine the characteris-

 0038-5301/92/03 0301-06 $03.00

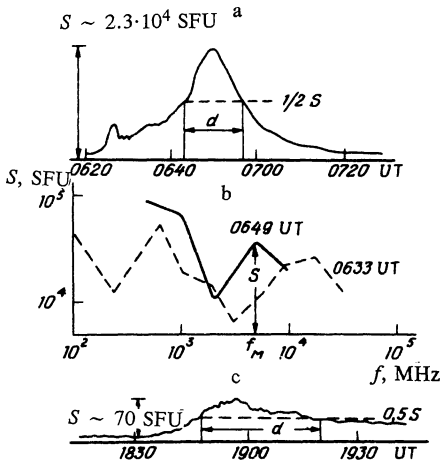

FIG. 1. Typical characteristics of radio bursts. Time profile (a) (3000 MHz, Institute of Terrestrial Magnetism, the Ionosphere, and Radio Propagation) and frequency spectrum (b) of a large radio burst on 12 Oct. 1981; time profile (c) of a prolonged burst of the "gradual rise and fall" (GRF) type on 23 Nov. 1980 (2800 MHz).

tic properties of electromagnetic radiation from events associated with CTs, we must also consider flares that were definitely not accompanied by CTs. Unfortunately, only about 30 such flares have been given in Refs. 4-6 and 11 for the P78-1 satellite. Even when observations were made, CTs from the central zone might not be detected because of the decrease in white-light luminosity as they ascend in the corona. In analyzing flares not accompanied by CTs, we must therefore also confine the analysis to limb events.

The velocities given in Refs. 4-6 and 9-13 for a CT front were determined from the "height–time" trajectory. derived from successive CT images or calculated from the location the bow part of the CT and the delay relative to the corresponding flare. The sizes of CTs in the plane of the sky were measured in degrees as the range $\Delta\theta$ of position angles occupied by the CT, and were determined mainly at the stage in which the entire CT was in the coronagraph field of view. The mass of a CT was estimated to be the product of its angular size $\Delta\theta$ and calibrated quantities characterizing the amount of matter in the line of sight per unit position angle for CTs of different brightness (see Refs. 13 and 14).

In determining the characteristics of the electromagnetic radiation, in addition to the data given in Refs. 4, 6, and 9-13 we made extensive use of information contained in Ref. 15. Here, in particular, we refer to the maximum flux and the total duration of the soft (1-8 Å) x-ray burst, as well as the absolute peak flux density S of the centimeter-wave burst at $f \geq 3$ GHz, its effective duration d at the $0.5S$ level, and the frequency f_m of the spectral maximum (Fig. 1). In most cases, d was measured from time profiles obtained at a number of observatories (see Refs. 15-17). In radio bursts with a complicated time profile consisting of several components, d was the sum of the durations of the individual components at a common $0.5S$ level for the entire burst. For some GRF bursts, which usually have a smooth time profile of simple shape (see Fig. 1c), d was determined from tables in Refs. 15-17 with allowance for the total duration and maximum and median radio fluxes. In those GRF bursts with an effective duration $d > 100$ min, the value $d \sim 100$ min was taken as the final value of that parameter. The laws discussed below that characterize the CT distribution in the "intensity–duration" diagram of a microwave burst remain valid and change little in a quantitative respect if, instead of the absolute maximum intensity S of the radio burst, one uses the flux at some fixed frequency, such as 3, 9, or 15 GHz.

CT ORIGIN AND ANGULAR SIZE

In Fig. 2 we give a diagram with universal coordinates for the present work: the absolute maximum flux density S of a microwave burst the vertical coordinate and the effective duration d of the radio burst the horizontal. The individual symbols in that plane denote events from the limb zone of heliolongitude $|l| \geq 45°$ that were accompanied by the corresponding CTs, according to Refs. 4-6 and 9-13, as well as events in a CT was determined to be absent. For events with a CT, the degree of blackening of the circles corresponds to increasing CT angular size. The range of angular size in this set of events was $\Delta\theta \sim$ 10-160° (see Ref. 14).

The distribution of events with different characteristics in the $(S-d)$ diagram clearly obeys certain laws, enabling one to identify a number of zones in which events with no CT and events with CTs of different angular size are concentrated. The boundaries of those zones that are shown in Fig. 2 are tentative, of course.

1) Events with a CT correspond mainly to radio bursts of two qualitatively different types: a) large unpulsed flares with a microwave emission intensity $S \geq 100$ SFU (solar flux units; 1 SFU = 10^{-22} W·m^{-2}·Hz^{-1}) and an effective burst duration $d >$ 1-2 min; b) bursts of relatively low intensity ($S \sim$ 10-100 SFU) but considerable duration ($d \geq 20$ min) – events of the GRF type.

2) A sharp cutoff of the effective duration of large centimeter-wave bursts associated with CTs is observed at $d \sim 20$ min, with the limit remaining at that level in bursts with

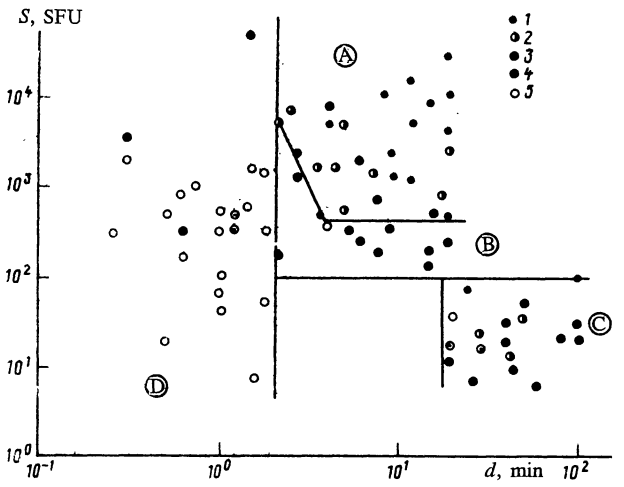

FIG. 2. Distribution in the "microwave burst intensity (S)–effective duration (d)" diagram of limb events with CTs of different angular sizes: 1) very large (≥90°); 2) large (60-90°); 3) moderate (30-60°); 4) small (<30°); 5) events with no CT. The tentative boundaries of the zones of intense (A), moderate (B), GRF (C), and pulsed (D) radio bursts are shown by lines.

intensities differing by more than two orders of magnitude. About the same d is the lower limit for the effective duration of GRF bursts in events with CTs.

3) In zone A, corresponding to the most intense ($S \geq 4 \cdot 10^2$-$5 \cdot 10^3$ SFU) and prolonged ($d >$ 2-4 min) radio bursts, CTs of large and very large size $\Delta\theta \geq 60°$ predominate (~85% out of 27). The largest CTs with $\Delta\theta \geq 90°$, comprising ~50% here, are concentrated mainly in the upper right-hand part of zone A.

4) In zone B of moderate microwave bursts ($S \sim$ 100-400 SFU for $d >$ 4 min and S up to $5 \cdot 10^3$ SFU for $d \sim$ 2-4 min), most of the CTs (9 out of 10) have a moderate angular size, $\Delta\theta \sim$ 30-60°. Several moderate CTs were also recorded in the lower left-hand part of zone A of intense bursts. The distribution of events in zones A and B and partially in zone D (see below) indicates, as a whole, a decrease in CT angular size with decreasing intensity and duration of flare microwave bursts with $S \geq 100$ SFU.

5) Events with prolonged GRF bursts (zone C), despite the relatively low radio intensity, are accompanied by CTs with a wide range of angular size. Moderate CTs with $\Delta\theta \sim$ 30-60° are also observed here in most events (~60% out of 18). Occasionally, however, large CTs with $\Delta\theta$ up to 100° were observed in conjunction with GRF bursts (five cases). The appearance of CTs of small angular size $\Delta\theta < 30°$ is also possible (two cases).

6) Zone D of pulsed and quasipulsed bursts with $d <$ 2 min can be characterized as a zone of events with no CT or with a CT of small angular size. Among the 23 events in this zone, only two CTs from the most powerful flares with pulsed energy release and $S > 4 \cdot 10^3$ SFU had moderate angular sizes in the range $\Delta\theta \sim$ 35-40°. In four other cases with $S \sim$ 250-1500 SFU, small CTs with $\Delta\theta < 30°$ were observed, and CTs were absent in the remaining 17 cases (i.e., ~74%).

A similar, although somewhat different, division of events is obtained when soft x-ray instead of microwave emission is used. In that case one considers a diagram of maximum flux F (x-ray class) vs total burst duration τ (Fig. 3). In zone A of the most intense, long-duration x-ray bursts (LDEs) of class from ≥M6 to ≥M2 and with $\tau > 2$ h, large CTs with $\Delta\theta = 60°$ predominate (22 out of 25 cases). In the intermediate zone B, which includes bursts of relatively short duration ($\tau \sim$ 1-2 h) and different intensities, as well as prolonged bursts (up to $\tau \sim$ 5 h) of classes from <M6 to <M2, most CTs (21 out of 27) are of moderate angular size, $\Delta\theta \sim$ 30-60°. In zone D of pulsed x-ray bursts with $\tau <$ 1 h, mainly events with no CT are observed (17 out of 24 flares). Only in certain cases, mainly of fairly high intensity ≥M3, might there be CTs of small (four cases) and moderate (three cases) angular size, $\Delta\theta \leq$ 30-40°.

The data on soft x rays given here confirm the well-known relationship between the duration of an x-ray burst, on the one hand, and the origin and angular size of CTs, on the other.[3,4,7] A significant refinement of the present analysis is that, as in the case of microwave emission, not only the duration of the bursts but also their intensity, i.e., the character of the flare energy release as a whole, is of great importance for these CT characteristics.

From a comparison of the analyses of CTs and bursts in the two ranges, it follows, in particular, that pulsed bursts,

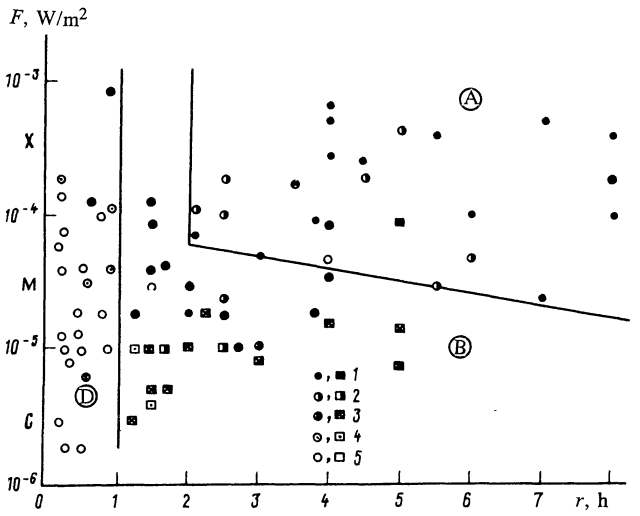

FIG. 3. Distribution in the "soft x-ray burst intensity (F)–total duration (τ)" diagram of limb CTs of different angular sizes (see Fig. 2). Events corresponding to GRF radio bursts are shown by squares. Zones of intense (A), moderate (B), and pulsed (D) soft x-ray bursts are shown.

which are observed in the centimeter range as bursts with $d \leq 2$ min, have a total duration $\tau \leq 1$ h in soft x rays. Moreover, in contrast to (S–d) radio diagrams, in the x-ray (F–τ) diagram events of the GRF type (squares in Fig. 3) are not isolated in a separate zone, although they are concentrated in the intermediate zone B, predominantly in the domain of relatively low flux (class ≤M2) and moderate duration ($\tau \sim$ 1-3 h). In soft x rays, events with GRF radio bursts are simply a special case of LDE events, which are characterized by low intensity and not the longest duration.

CT PARAMETERS AND BURST CHARACTERISTICS

Using a similar approach, we analyze the relationship between other CT parameters (velocity, mass, and shape) and the characteristics of microwave and soft x-ray bursts. As before, we confine ourselves to the analysis of CTs associated with flares at heliolongitudes $|l| \geq 45°$. In the analyzed set of events, the CT velocity and mass are in the ranges $V \sim$ 300-1700 km/sec and $m \sim 3 \cdot 10^{14}$-$3 \cdot 10^{16}$ g (see Ref. 14). Three and five CT categories have been identified with respect to these parameters, respectively. The CTs can be grouped with respect to the complexity of their observed shape as: single and double spikes; multiple spikes and a fan; curved front and loops; filled loops, clouds, and remnants of large CTs.

The analysis shows that in the standard radio (S–d) and x-ray (F–τ) diagrams, CTs with different velocities, masses, and shapes are also concentrated in certain zones, similar in their arrangement to the zones of intense (A), moderate (B), GRF (C), and pulsed (D) bursts identified in the analysis of CT angular size (see Figs. 2 and 3). Here it is sufficient to introduce only slight changes into the boundary between zones A and C, particularly for microwave bursts with an effective duration $d \sim$ 2-4 min. In this case it is convenient to represent the results as histograms characterizing the distribution of CTs with certain parameters in each of the zones.

From Figs. 4 and 5, in which such histograms are shown, it is clear that in both ranges over all three parame-

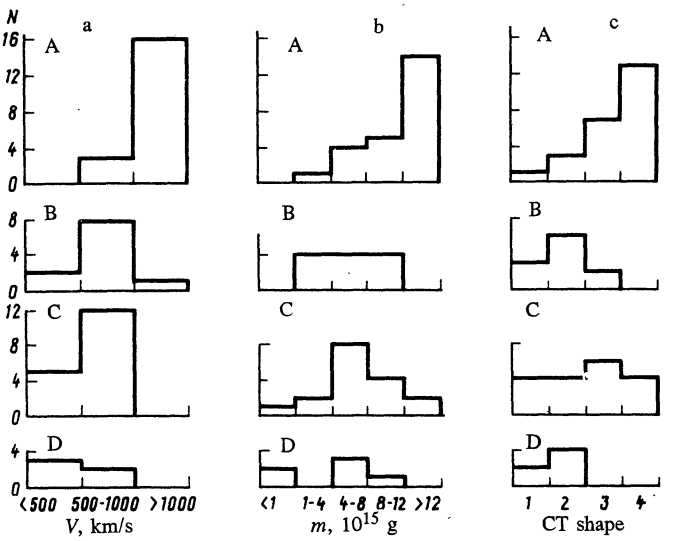

FIG. 4. Distribution of CTs with respect to velocity (a), mass (b), and shape (c) for zones of intense (A), moderate (B), GRF (C), and pulsed (D) microwave bursts (see Fig. 2). The CT shapes (c) are classified as 1) single and double spikes; 2) multiple spikes, fans; 3) curved front, loops; 4) filled loops, clouds, remnants of complicated CTs.

ters (velocity, mass, and shape) there are significant differences between the respective zones, especially between the zones of intense (A) and moderate (B) bursts. The trend toward a decrease in velocity and mass and a simplification of the shape of CTs between zone A and zones B and D, i.e., with decreasing intensity and duration of microwave and x-ray bursts, is obvious; radio bursts of the GRF type (zone C) are associated with CTs that mainly have moderate characteristics. In combination with the data on the angular sizes of CTs and the other results of the present analysis, this enables us to draw the following conclusions.

1) The parameters of microwave and soft x-ray bursts, particularly the combination of intensity and effective duration, reveal a close relationship to the origin and characteristics of the corresponding CTs. In burst intensity–duration diagrams there are zones that enable one to distinguish between events with and without CTs having different angular size, velocity, mass, and shape.

2) Pulsed flares with centimeter-wave bursts of effective duration $d < 2$ min or soft x-ray bursts of total duration $\tau <$ 1 h are not accompanied by CTs, as a rule. Only the most intense pulsed bursts may be associated with CTs of the spike or fan type with a small angular size $\Delta\theta \leq$ 30-40°, a moderate velocity $V \sim$ 350-400 km/sec, and small or moderate mass $m \sim 5 \cdot 10^{14}$-10^{16} g.

3) Moderate microwave bursts ($d \sim$ 2-4 min at $S \geq 100$ SFU and $d >$ 4 min at $S \sim$ 100-400 SFU) and moderate soft x-ray bursts ($\tau \sim$ 1-2 h in any class, as well as $\tau \sim$ 2-8 h in classes from ≤M7 to ≤M2) correspond most often to CTs of relatively simple shape (usually spikes, fans, loops, and sometimes a curved front) and moderate angular size ($\Delta\theta \sim$ 30-60°), velocity ($V \sim$ 400-1000 km/sec), and mass [$m \sim$ (1-10)·10^{15} g].

4) The most intense and prolonged microwave ($S >$ 400 SFU at $d \geq$ 4 min) and x-ray (classes from >M7 to >M2 at $\tau \geq$ 2 h) bursts are associated with the largest ($\Delta\theta \geq$ 60-90°), highest-velocity ($V \geq$ 1000 km/sec), and massive [$m \geq$ (8-12)·10^{15} g] CTs of complicated shape (curved front, filled loop, or remnants of large CTs).

5) In the radio, ~30% of CTs are associated with relatively weak ($S <$ 100 SFU) and prolonged ($d \geq$ 20 min) bursts of the nonexplosive GRF type. For such events, CTs with moderate characteristics are the most typical, although the range of possible CT parameters is fairly broad.

6) The CTs of different shapes differ not only in angular size, velocity, and mass, but also in the characteristics of their microwave and x-ray emission. This indicates that the different CT shapes observed in white light reflect actual physical differences between the mass ejections, rather than being a consequence only of geometrical or other similar factors (see Ref. 18).

7) We note one other result, which we have not described in detail here but which was obtained in the present analysis. An examination of the complete set of events, including flares over the entire visible disk, shows that many microwave bursts from zones A and B, which have an effective duration $d \geq$ 6 h and are accompanied by large CTs, are characterized by a soft frequency spectrum with the maximum flux density at $f_m \sim$ 3-5 MHz, and the corresponding x-ray bursts are of relatively low intensity.

DISCUSSION

What do these regularities mean from the standpoint of our present understanding of the origin of CTs and their relationship to flare energy release?

There is obviously a definite relationship between the parameters of CTs and flares, but that relationship is not very simple. By a flare we usually mean a rapid release of energy, stored in the nonpotential component of the magnetic field above an active region, for example, that occurs by means of magnetic reconnection in a current sheet, is accompanied by particle acceleration, plasma heating, and magnetohydrodynamic motion, and is manifested in the form of secondary effects – various kinds of emission, in particular (see Ref. 19). The eruption of a CT may also be a consequence of an

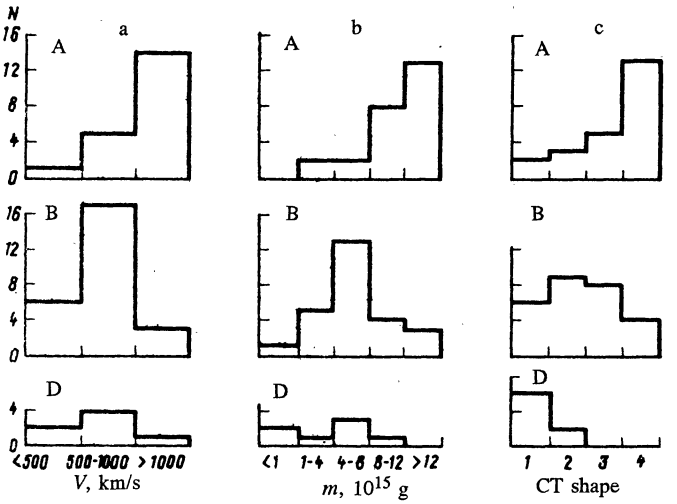

FIG. 5. Same distributions as in Fig. 4, for zones of intense (A), moderate (B), and pulsed (D) soft x-ray bursts (see Fig. 2).

overall disturbance in the equilibrium of the evolving magnetosphere above an active region or of its individual structures – of prominences or filaments, in particular.[20,21] Hence it follows that depending on the specific conditions, CTs and flares may either occur independently or exhibit a close interrelationship.

As we demonstrated above, in most pulsed (compact) flares of moderate intensity, energy is generally released without a visible CT. Magnetic reconnection and the corresponding energy release in those events may be caused by other factors independent of CTs, such as the upwelling of new magnetic flux, the interaction of loops, etc.

In cases in which both CTs and flares are observed, situations are possible in which the CT eruption initiates a flare, and in which the origin and ascent of the CT is a response to flare energy release. According to Ref. 8, the eruption of a loop-shaped CT begins with the ascent of the cavity of a prominence in the stage of the precursor of an x-ray (or radio) burst. As it moves, the CT deforms the magnetic field structure and then causes flare energy release near one base of the loop of the transient. Such a sequence of events, however, is probably typical only of relatively weak and simple flares.

In large prolonged flares with well-developed space–time structure, a more complicated relationship between the flare and the CT eruption certainly exists, resulting in multiple energy release in different parts of the magnetosphere above the active region. The observed relationship between the parameters of the microwave (x-ray) bursts and the CT is then due to the fact that the eruption of large, massive, and high-velocity CTs is associated with strong and prolonged energy release, including the acceleration of a large number of particles.

It must be specially stressed that prolonged energy release in the stage of formation of the post-flare system of loops, when the CT is already at a large height above the photosphere, and the magnetic field structure disturbed by it above the active region relaxes toward its initial state,[22,23] may also contribute significantly to the relationship between the characteristics of CTs and microwave (x-ray) bursts under consideration. Such relaxation also occurs by means of magnetic reconnection with the formation of a vertical current sheet, is accompanied by prolonged particle acceleration, and results in the generation of LDE bursts in soft x rays and prolonged microwave bursts with a soft frequency spectrum (see Ref. 2). Recall that just such a soft radio spectrum is observed in many flares associated with large CTs.

The eruption of CTs, including moderate and even large ones, is not always associated with explosive energy release, however. In relatively weak magnetic fields in the absence of the appropriate conditions in the active region, the eruption of a prominence, the instability of other large-scale structures, and the ascent of a CT leads not so much to particle acceleration as to prolonged plasma heating in the lower corona, particularly as the magnetic field relaxes toward its initial state. This stage must obviously be present in all events with the eruption of a fairly large CT. In those cases, energy release is manifested in bursts of relatively moderate intensity with a weak pulsed phase, or prolonged microwave emission of the "gradual rise and fall" (GRF) type. Approximately such emission, or even weaker, in microwaves and soft x rays is accompanied by CTs that are associated with the disappearance of filaments outside active regions.

Finally, there is reason to believe that there is a class of CTs (mainly small and low-energy), whose origin and ascent almost never show up in the x-ray, microwave, or visible.[24]

Thus, there is a broad spectrum of events with different relationships between CT eruption and flare or flare-like energy release, with the variations in that relationship being reflected quite definitely in the character (intensity, duration, and spectrum) of the microwave and x-ray bursts. The laws indicated above should be taken into account in developing appropriate physical models. They also lay the groundwork for electromagnetic diagnostics of flare CTs.

We thank T. S. Podstrigach (Scientific Research Radiophysics Institute), V. A. Senik (GAS, Main Astronomical Observatory), N. N. Potapov and L. M. Bakunin (Siberian Branch of the Institute of Terrestrial Magnetism, the Ionosphere, and Radio Propagation), H. Aurass (Tremsdorf, Germany), O. Alvarez and E. Del Poso (Havana, Cuba), A. Magun and R. Hermann (Bern, Switzerland), V. Gaizauskas (Ottawa, Canada), C. Enome and K. Shibasaki (Toyokawa, Japan), and T. Kosugi (Nobeyama, Japan) for the opportunity to analyze original time profiles of radio bursts. We are grateful to B. Rompolt (Wrocław University, Poland) for useful consultations, as well as D. J. Michels, R. A. Howard, M. J. Koomen, and N. R. Sheeley, Jr. (Naval Research Laboratory, USA), authors of the experiment on CT observations using the SOLWIND coronagraph on the P78-1 satellite, which provides data for the present analysis.

[1]S. Kahler, *Rev. Geophys.* **25**, 663 (1987).
[2]I. M. Chertok, *Astron. Zh.* (1992) (in press).
[3]N. R. Sheeley, Jr., R. A. Howard, M. J. Koomen, et al., *Astrophys. J.* **277**, 349 (1983).
[4]N. R. Sheeley, Jr., R. T. Stewart, R. D. Robinson, et al., *Astrophys. J.* **279**, 839 (1984).
[5]S. Kahler, N. R. Sheeley, Jr., R. A. Howard, et al., *Sol. Phys.* **93**, 133 (1984).
[6]R. D. Robinson, R. T. Stewart, N. R. Sheeley, Jr., et al., *Sol. Phys.* **105**, 149 (1986).
[7]S. W. Kahler, N. R. Sheeley, Jr., and M. Liggett, *Astrophys. J.* **344**, 1026 (1989).
[8]R. A. Harrison, E. Hildner, A. J. Hundhausen, et al., *J. Geophys. Res.* **95**, 917 (1990).
[9]N. R. Sheeley, Jr., R. A. Howard, M. J. Koomen, et al., *J. Geophys. Res.* **90**, 163 (1985).
[10]S. W. Kahler, E. W. Cliver, N. R. Sheeley, Jr., et al., *J. Geophys. Res.* **90**, 177 (1985).
[11]S. W. Kahler, N. R. Sheeley, Jr., R. A. Howard, et al., *J. Geophys. Res.* **89**, 9683 (1984).
[12]E. W. Cliver, I. D. Mihalov, N. R. Sheeley, Jr., et al., *J. Geophys. Res.* **92**, 8487 (1987).
[13]H. V. Cane, N. R. Sheeley, Jr., and R. A. Howard, *J. Geophys. Res.* **92**, 9869 (1987).
[14]R. A. Howard, N. R. Sheeley, Jr., M. J. Koomen, et al., *J. Geophys. Res.* **90**, 8173 (1985).
[15]*Solar-Geophysical Data,* NOAA, Boulder (1979-1982).
[16]*Atlas of Solar Radio Emission, 1979-1982,* Toyokawa Obs., WDC-2 (1981-1989).